Quark-gluon vertex with 2 flavours of O(a) improved Wilson fermions

Ayşe Kızılersü,[a] **Orlando Oliveira,**[b] **Paulo Silva,**[b] **Jon-Ivar Skullerud**[c,*] **and André Sternbeck**[d]

[a]*CSSM, Department of Physics, Faculty of Sciences, School of Physical Sciences, University of Adelaide, 5005, Adelaide, Australia.*

[b]*CFisUC, Department of Physics, University of Coimbra, 3004–516 Coimbra, Portugal.*

[c]*Department of Theoretical Physics, National University of Ireland Maynooth, Maynooth, County Kildare, Ireland.*

[d]*Theoretisch-Physikalisches Institut and Universitätsrechenzentrum, Friedrich-Schiller-Universität Jena, 07743 Jena, Germany*

E-mail: jonivar.skullerud@mu.ie

We study the Landau-gauge quark-gluon vertex with 2 flavours of $O(a)$ improved Wilson fermions, for several lattice spacings and quark masses. In the limit of vanishing gluon momentum, we find that all nonzero form factors have a significant infrared strength, and that the leading form factor λ_1, multiplying the tree-level vertex structure, is significantly enhanced in the infrared compared to the quenched case. We find that all form factors are further enhanced in the infrared as the chiral and continuum limits are approached.

The 38th International Symposium on Lattice Field Theory, LATTICE2021 26th-30th July, 2021
Zoom/Gather@Massachusetts Institute of Technology

---

*Speaker

1. Introduction

The quark–gluon vertex is one of the basic ingredients of QCD, along with the gluon and quark propagators and the three-gluon and four-gluon vertices. It encodes the fundamental interaction between quarks and gluons, and as such lends itself naturally to defining an effective charge (running coupling). It is also a crucial ingredient in the gap equation (Dyson–Schwinger equation) for the quark propagator. Indeed, its role in this equation and its relation to dynamical chiral symmetry breaking (DχSB) and quark confinement provides a compelling reason to study it in more detail.

Since the nonperturbative quark and gluon propagators (at least in Landau gauge) are by now very well known, it is clear that consistent results, including a sufficient level of DχSB and adequate meson phenomenology, cannot be obtained with a bare vertex or indeed a vertex constructed from the abelian Ward–Takahashi identity. In particular, vertex structures beyond the one found at tree level are crucial to obtaining the correct phenomenology.

In recent years there has been significant progress in our understanding of the quark–gluon vertex using functional methods and constraints from the longitudinal and transverse Slavnov–Taylor identities (see for example [1–5]). There has only been a very small number of lattice calculations, mostly in the quenched approximation [6–9]. Here we report on and update a recent calculation with $N_f = 2$ dynamical fermions and several lattice spacings and quark masses [10].

2. Calculation details

2.1 Lattice parameters

We have used gauge ensembles from Regensburg QCD (RQCD) collaboration [11], with $N_f = 2$ nonperturbatively clover-improved Wilson fermions. The parameters used are listed in Table 1. In addition to the RQCD ensembles, we have produced a quenched ensemble with lattice spacing $a = 0.07$ fm (matching the L07 and H07 ensembles), but with a larger valence quark mass $m_\pi \approx 1000$ MeV. The configurations have been fixed to Landau gauge using an overrelaxation algorithm. More details can be found in [10].

Name	β	κ	a [fm]	V	m_π [MeV]	N_{cfg}	N_{src}
L08	5.20	0.13596	0.081	$32^3 \times 64$	280	900	4
H07	5.29	0.13620	0.071	$32^3 \times 64$	422	900	4
L07	5.29	0.13632	0.071	$32^3 \times 64$	295	908	4
L07-64	5.29	0.13632	0.071	$64^3 \times 64$	290	750	2
H06	5.40	0.13647	0.060	$32^3 \times 64$	426	900	4
Q07	6.16	0.1340	0.071	$32^3 \times 64$	1000	998	4

Table 1: Lattice ensembles and parameters used in this study.

We have used the same clover action for the valence quarks as for the sea quarks, with an off-shell $O(a)$-improved "rotated" quark propagator,

$$S_R(x, y) = \left\langle (1 + b_q am)^2 (1 - c_q a \overrightarrow{\slashed{D}}(x)) M^{-1}(x, y; U)(1 + c_q a \overleftarrow{\slashed{D}}(y)) \right\rangle , \tag{1}$$

2

where $M(x, y; U)$ is the fermion matrix evaluated on a single gauge configuration U. The quark–gluon vertex is then determined after Fourier transforming by

$$\Lambda_\mu^{a,\text{lat}}(p, q) = S_R(p)^{-1} \left\langle\!\left\langle S_R(p; U) A_\mu^a(q) \right\rangle\!\right\rangle S_R(p + q)^{-1} D(q)_{\nu\mu}^{-1}, \tag{2}$$

where $\left\langle\!\left\langle \cdot \right\rangle\!\right\rangle$ denotes averaging over gauge fields only, while $S_R(p; U)$ is the Fourier transform of (1) evaluated on a single gauge configuration U.

2.2 Extracting form factors

The one-particle irreducible quark-gluon vertex, $(\Lambda_\mu^a)_{\beta\rho}^{ij} = t_{ij}^a (-i g_0 \Gamma_\mu)_{\beta\rho}$, can be written in terms of 12 independent tensor structures in a general kinematics. Here we will consider only the soft gluon kinematics, where the gluon momentum is zero, and hence the vertex depends only on the quark momentum p. In this kinematics, the quark–gluon vertex can be expressed in terms of three independent tensor structures with associated form factors $\lambda_{1,2,3}$,

$$\Gamma_\mu(p) = \lambda_1(p^2)\gamma_\mu + 4\lambda_2(p^2)\slashed{p} p_\mu + 2i\lambda_3(p^2)p_\mu. \tag{3}$$

From (3), we derive the following expressions which may be used to determine the form factors λ_i,

$$\lambda_1 = \frac{1}{3}\left(\delta_{\mu\nu} - \frac{p_\mu p_\nu}{p^2}\right) \text{Tr}_4 \, \gamma_\nu \Gamma_\mu, \tag{4}$$

$$\lambda_2 = \frac{1}{12p^2}\left(\delta_{\mu\nu} - 4\frac{p_\mu p_\nu}{p^2}\right) \text{Tr}_4 \, \gamma_\nu \Gamma_\mu, \tag{5}$$

$$\lambda_3 = \frac{p_\mu}{2i p^2} \text{Tr}_4 \, \Gamma_\mu. \tag{6}$$

In addition to these *covariant* expressions we also employ the following *non-covariant* expressions for λ_1, λ_2,

$$\lambda_1 = \text{Tr}_4 \, \gamma_\mu \Gamma_\mu \Big|_{p_\mu=0}, \tag{7}$$

$$\lambda_2 = \frac{p_\mu p_\nu}{4p^2} \text{Tr}_4 \, \gamma_\nu \Gamma_\mu \Big|_{\nu\neq\mu}. \tag{8}$$

In [10] only the non-covariant expressions were used. Here we will also present results using the covariant expressions. We note that these were previously used in [8].

2.3 Tree-level correction

The tree-level rotated vertex in the soft gluon kinematics is given by

$$\Gamma_\mu^{(0)}(p, 0, p) = \frac{1}{\left(1 + c_q^2 a^2 K^2(p)\right)^4}\bigg\{\gamma_\mu \left[\left(1 + c_q^2 a^2 K^2(p)\right)^2 C_\mu(p)\right]$$
$$-4a^2 K_\mu \slashed{K}(p) \left[2c_q^2 C_\mu(p) - c_q\left(1 - c_q^2 a^2 K^2(p)\right)\right]$$
$$-2ia K_\mu \left[-2c_q^2 a^2 K^2(p) + \frac{1}{2}\left(1 - c_q^2 a^2 K^2(p)\right)\right.$$
$$\left.- 2c_q\left(1 - c_q^2 a^2 K^2(p)\right) C_\mu(p)\right]\bigg\}, \tag{9}$$

3
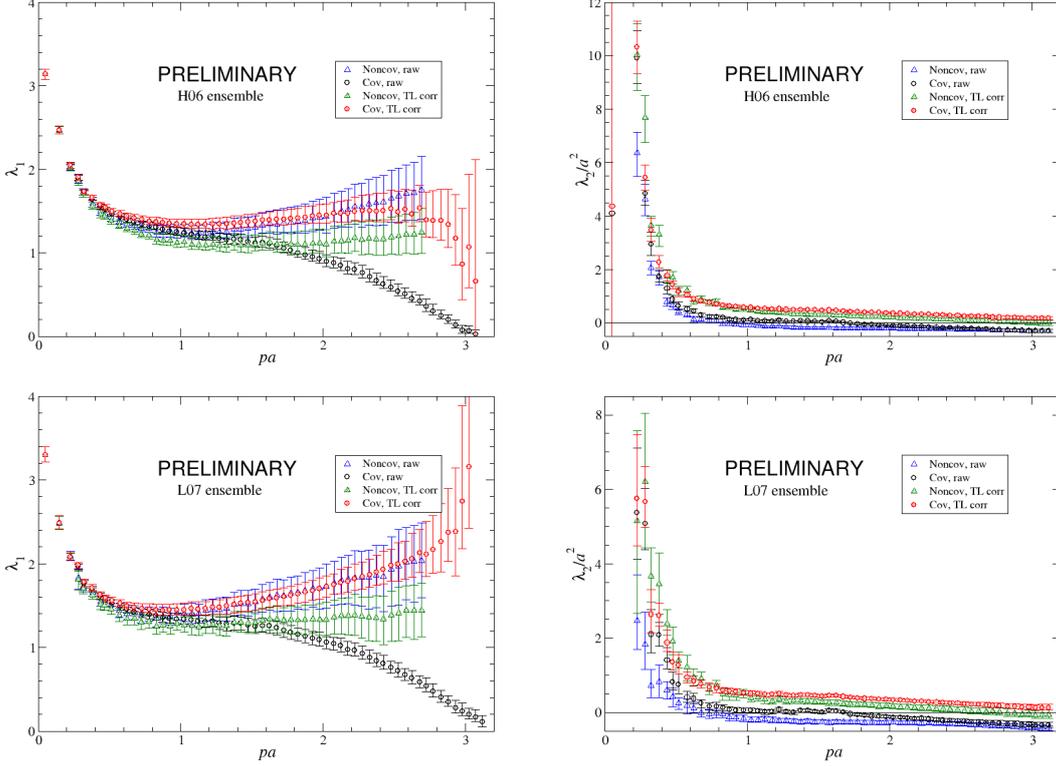
Figure 1: Comparison of covariant and non-covariant determination of λ_1 (left) and λ_2 (right) from the H06 (top) and L07 (bottom) ensembles, with and without tree-level correction. The data have not been renormalised.

where the lattice momentum variables K_μ, C_μ are given by

$$K_\mu(p) = \frac{1}{a}\sin(p_\mu a)\,, \qquad\qquad C_\mu(p) = \cos(p_\mu a)\,. \qquad (10)$$

From this we note that all three form factors have a nontrivial momentum dependence already at tree level on the lattice, and we correct for this by dividing the raw lattice data for λ_1 (which is 1 at tree level in the continuum) by its tree-level form, while for λ_2 and λ_3 (which are zero at tree level in the continuum) we subtract off the tree-level expressions from (9). The tree-level form also suggests replacing the Fourier transform momentum p with the lattice momentum $K(p)$ in (4)–(8). The detailed procedure for extracting and tree-level correcting the form factors is presented in [10].

3. Results

In figure 1 we compare the covariant [eqs (4), (5)] to the non-covariant [eqs (7), (8)] extraction of λ_1 and λ_2, for the H06 and L07 ensembles, with and without tree-level correction. We see that the results for λ_1 agree perfectly in the infrared, but diverge for $pa \gtrsim 0.5$. This is in part due to the tree-level correction: the uncorrected (raw) data agree for $pa \lesssim 1$, but the non-covariant λ_1 is brought down by the tree-level correction, while the covariant λ_1 is brought up. In the ultraviolet,

4
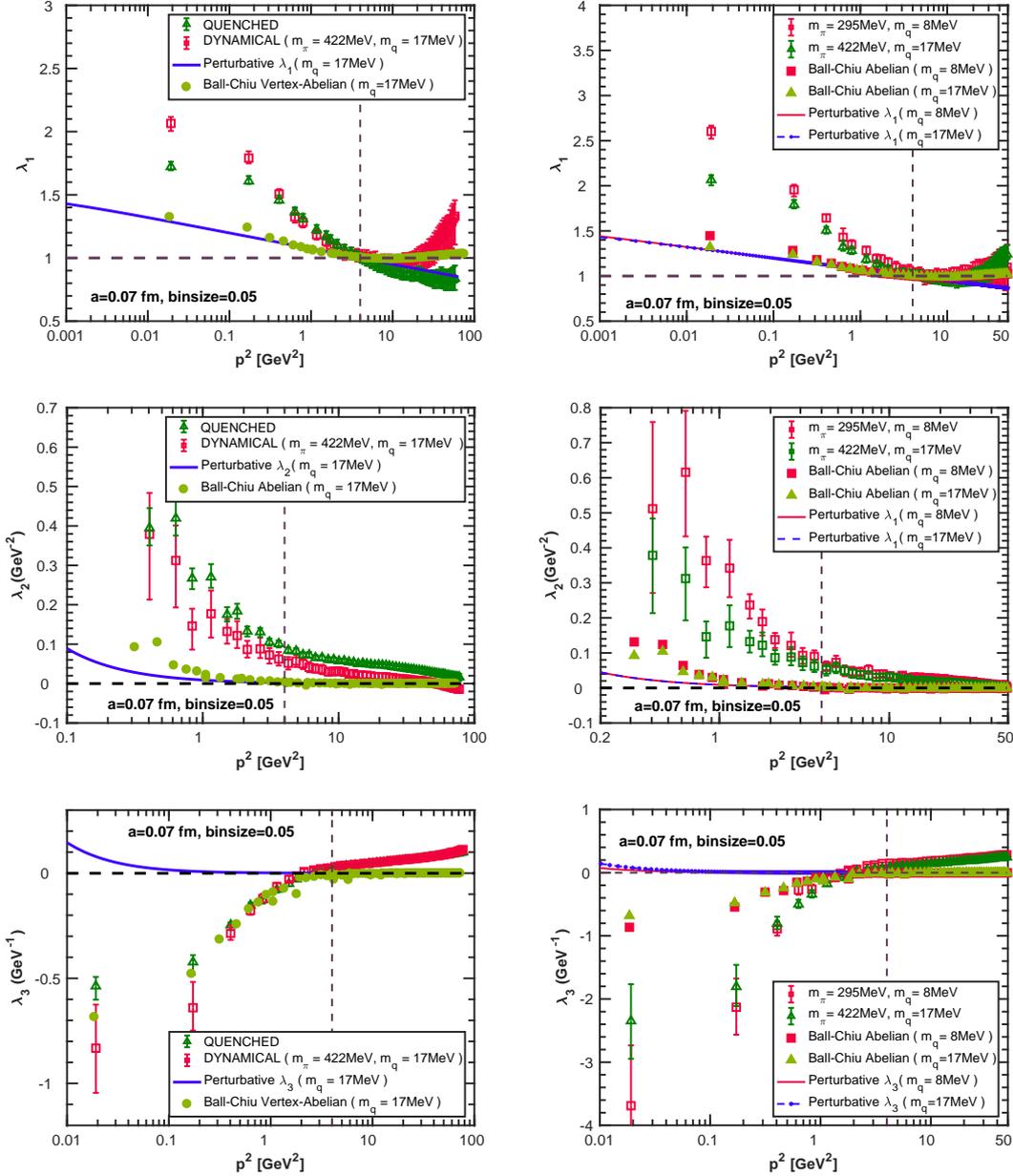
Figure 2: Quark mass and flavour dependence of (top to bottom) λ_1, λ_2 and λ_3. The left panel compares the Q07 (quenched) and H07 (dynamical) ensemble, while the right panel compares the L07 and H07 ensembles. Also shown are the 1-loop perturbative result as well as the Ball–Chiu vertex which satisfies the abelian Ward–Green–Takahashi identity.

the covariant λ_1 goes to zero at tree level, and this is also seen in the raw data. The tree-level corrected, covariant λ_1 therefore becomes very noisy in the UV.

In the case of λ_2, the covariant and non-covariant determinations agree very well after tree-level corrections for $pa \lesssim 1$, while in the ultraviolet the covariant data fall off somewhat more slowly than the non-covariant ones.

In figure 2 we compare the results for the form factors $\lambda_1, \lambda_2, \lambda_3$, renormalised at 2 GeV, for the Q07 (quenched), H07 and L07 ensembles. All these have the same lattice spacings, but differ in their quark flavour content. In the left panel, comparing the Q07 to the H07 ensemble, we see that the dynamical fermions have a moderate effect on all three form factors, and that including the sea quarks tends to enhance all of the form factors in the infrared. In the right panel we compare the H07 and L07 ensembles, which differ only by their quark mass. We see a similar effect, where the lighter quark gives a stronger enhancement in the infrared.

Next, in figure 3 we compare the form factors at different lattice spacings for the same physical quark mass. For the lighter quarks (L07 and L08) we see very little lattice spacing dependence, while for the heavier quarks (H06 and H07) a clear enhancement in the infrared is seen for all form factors as we approach the continuum limit.

Finally, in figure 4 we show the results from all our $N_f = 2$ ensembles, together with the earlier quenched results from [7]. The earlier results were obtained using a mean-field (tadpole) improved rather than a nonperturbatively determined clover coefficient, with a lattice spacing of 0.093 fm and a valence quark mass corresponding to $m_\pi \approx 880$ MeV [12]. We find good agreement with the old results, suggesting once again that quenching, lattice spacing and quark mass effects are moderate.

4. Outlook

We have presented results for the quark–gluon vertex in the soft gluon limit with two flavours of $O(a)$-improved Wilson fermion. The results are consistent with previous results in the quenched approximation, showing moderate dependence on flavour content, quark mass and lattice spacing in the range studied here. We have employed two different methods (covariant and non-covariant) to extract the form factors λ_1 and λ_2, and the results are consistent in the infrared. There is some discrepancy between the two methods for λ_1 at mid-momentum which still needs to be understood.

Our next step will be to compute the vertex in more general kinematics, which will give access to the full set of 12 form factors. Recent studies based on Dyson–Schwinger equations and exploiting Slavnov–Taylor identities [2, 4] suggest that only a few of these form factors give a significant contribution to the strength of the vertex, and our calculations will aim to check these findings.
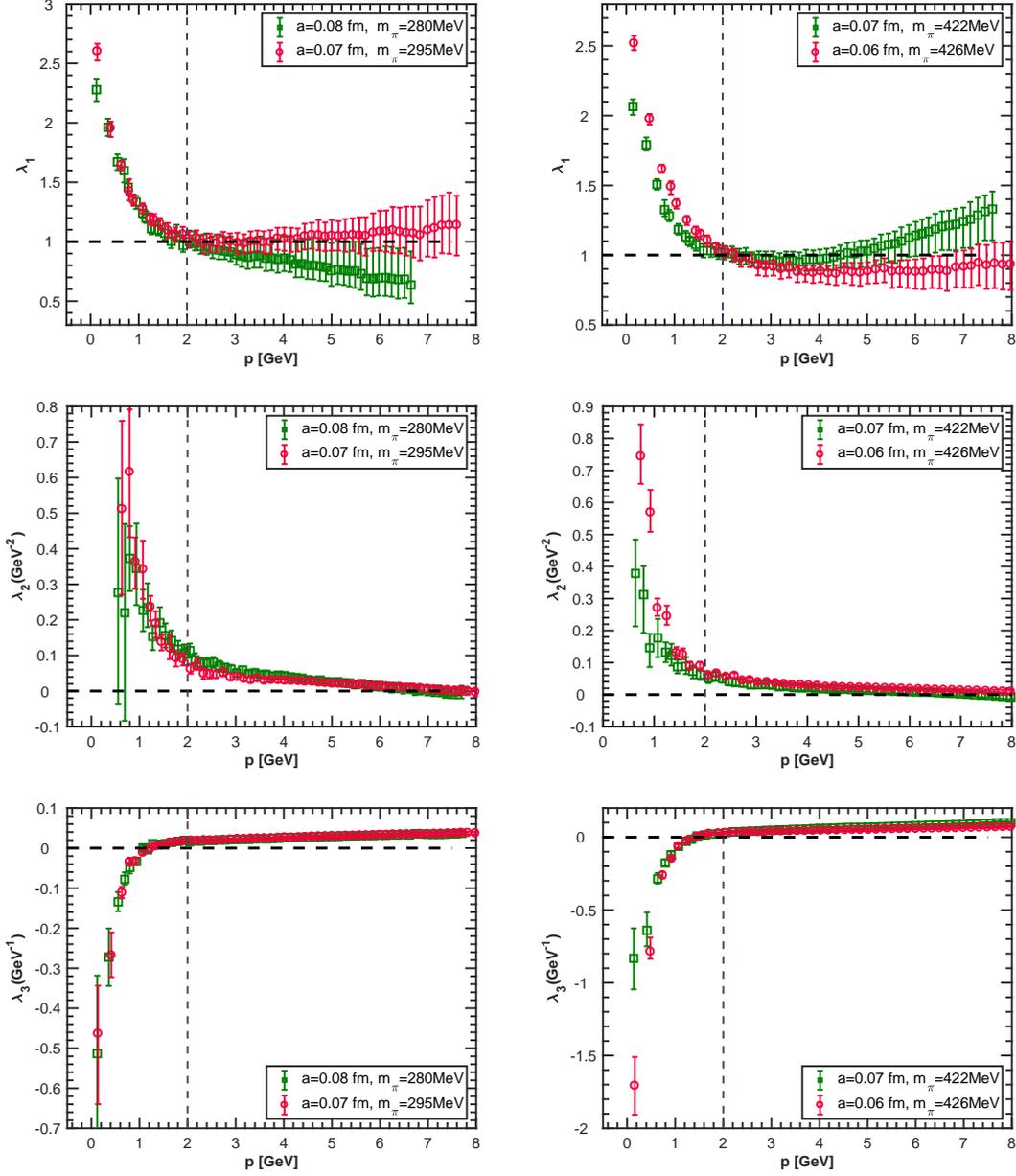
Figure 3: Lattice spacing dependence of (top to bottom) λ_1, λ_2 and λ_3. The left panel compares the L08 and L07 ensembles, while the right panel compares the H07 and H06 ensembles.

References

[1] R. Williams, C. S. Fischer and W. Heupel, *Light mesons in QCD and unquenching effects from the 3PI effective action*, *Phys. Rev. D* **93** (2016), no. 3 034026 [arXiv:1512.00455].
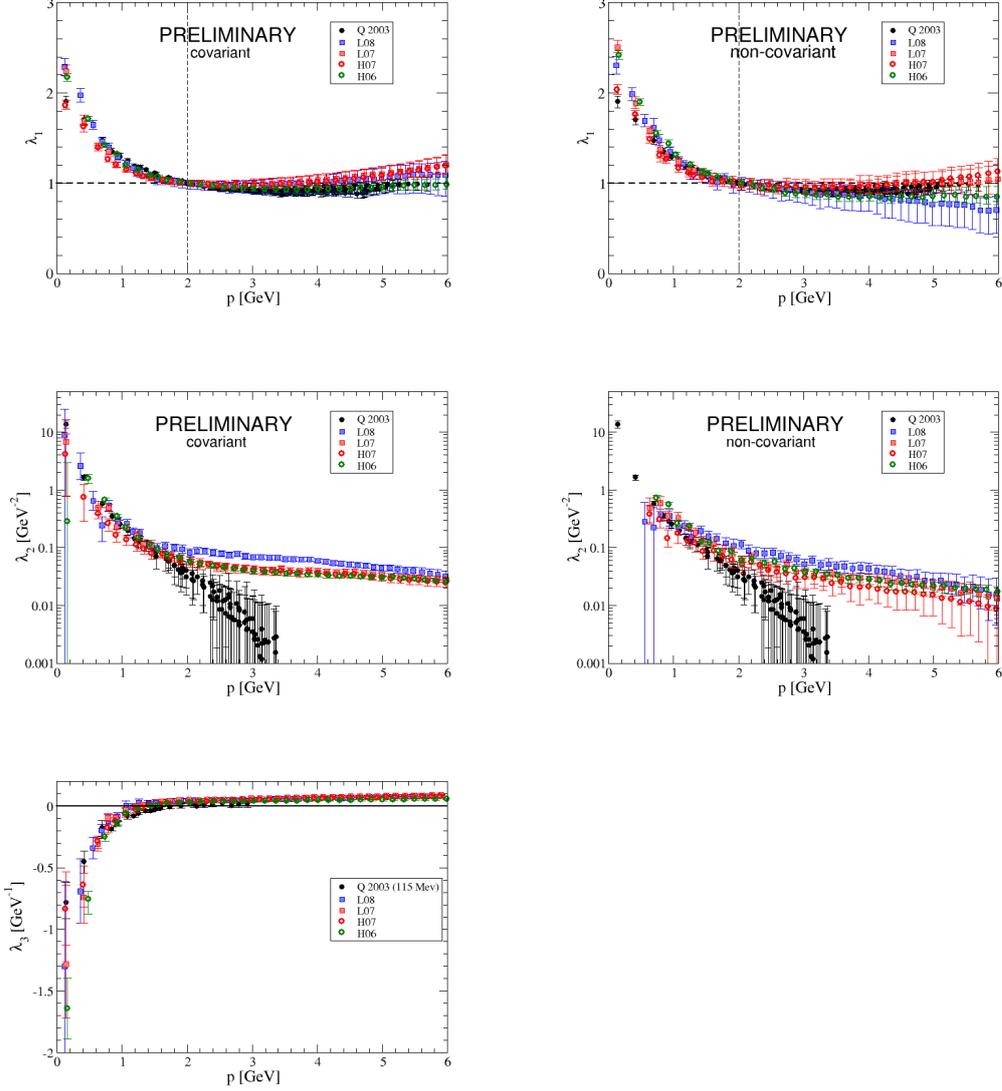
Figure 4: All form factors, renormalised at $\mu = 2\,\text{GeV}$, compared with the quenched results from 2003 [7], labelled "Q 2003". Left: covariant extraction; right: non-covariant extraction.

[2] D. Binosi, L. Chang, J. Papavassiliou, S.-X. Qin and C. D. Roberts, *Natural constraints on the gluon-quark vertex*, *Phys. Rev.* **D95** (2017), no. 3 031501(R) [arXiv:1609.02568].

[3] A. C. Aguilar, J. C. Cardona, M. N. Ferreira and J. Papavassiliou, *Quark gap equation with non-abelian Ball–Chiu vertex*, *Phys. Rev.* **D98** (2018), no. 1 014002 [arXiv:1804.04229].

[4] F. Gao, J. Papavassiliou and J. M. Pawlowski, *Fully coupled functional equations for the quark sector of QCD*, *Phys. Rev. D* **103** (2021), no. 9 094013 [arXiv:2102.13053].

[5] L. Albino, A. Bashir, B. El-Bennich, E. Rojas, F. E. Serna and R. C. da Silveira, *The impact*

of transverse Slavnov–Taylor identities on dynamical chiral symmetry breaking, arXiv:2108.06204.

[6] J.-I. Skullerud and A. Kızılersü, *Quark-gluon vertex from lattice QCD*, *JHEP* **09** (2002) 013 [hep-ph/0205318].

[7] J.-I. Skullerud, P. O. Bowman, A. Kızılersü, D. B. Leinweber and A. G. Williams, *Nonperturbative structure of the quark gluon vertex*, *JHEP* **04** (2003) 047 [hep-ph/0303176].

[8] H.-W. Lin, *Quark-gluon vertex with an off-shell O(a)-improved chiral fermion action*, *Phys. Rev. D* **73** (2006) 094511 [arXiv:hep-lat/0510110].

[9] A. Kızılersü, D. B. Leinweber, J.-I. Skullerud and A. G. Williams, *Quark-gluon vertex in general kinematics*, *Eur. Phys. J. C* **50** (2007) 871–875 [arXiv:hep-lat/0610078].

[10] A. Kızılersü, O. Oliveira, P. J. Silva, J.-I. Skullerud and A. Sternbeck, *Quark-gluon vertex from $N_f = 2$ lattice QCD*, *Phys. Rev. D* **103** (2021), no. 11 114515 [arXiv:2103.02945].

[11] G. S. Bali, S. Collins, B. Gläßle, M. Göckeler, J. Najjar, R. H. Rödl, A. Schäfer, R. W. Schiel, A. Sternbeck and W. Söldner, *The moment $\langle x \rangle_{u-d}$ of the nucleon from $N_f = 2$ lattice QCD down to nearly physical quark masses*, *Phys. Rev.* **D90** (2014), no. 7 074510 [arXiv:1408.6850].

[12] **UKQCD** Collaboration, K. C. Bowler *et. al.*, *Quenched QCD with O(a) improvement. 1. the spectrum of light hadrons*, *Phys. Rev. D* **62** (2000) 054506 [arXiv:hep-lat/9910022].